A Shock Tube Driven Transonic Wind Tunnel

J. Nash[a, b] *and B.W. Skews*[b]

Received 28 November 2012, in revised form and accepted 20 March 2013

A small transonic wind tunnel was designed, constructed and calibrated in order to provide a tool for the study and demonstration of transonic flow phenomena. The wind tunnel makes use of flow properties following the propagation of a shock wave along a tube in order to create the transonic flow. This is in contrast to conventional transonic facilities which are supplied from a reservoir or compressor through a nozzle. An RAE2822 aerofoil was used as the test piece due to the large amount of aerodynamic data available on it, especially in the transonic flow region, thus making it an excellent tool for validation. In addition, numerical simulations were conducted for comparison with the experiments. The short duration test time, which is determined by the tube length, was found to be adequate for establishing semi-steady state flow for a range of transonic flow Mach numbers. The results obtained experimentally compare well to results obtained numerically. The need for the addition of sophisticated instrumentation is identified.

Additional keywords: CFD, flow separation, Fluent©

Nomenclature

a	speed of sound
M	Mach number
p	pressure
γ	specific heat ratio

Subscripts

1	initial condition in driven section of tube
2	conditions behind the shock
3	conditions behind the contact surface
4	initial condition in driver section of tube
s	incident shock

1. Introduction

There are a wide variety of forms that wind tunnels can take, with each form providing specific advantages and disadvantages. However, with most wind tunnels a key objective in their design is to try and reproduce unbounded airflow such as that found when a body is exposed to airflow without nearby solid boundaries. In such a case, the streamlines around the body would bend and only become straight again at a theoretical infinite distance away. In a laboratory where space is limited there has to be a wind tunnel wall or some similar boundary at some finite distance from a test model which forces the streamlines to become straight again. During wind tunnel testing at high subsonic, sonic, or supersonic flow velocities, shock waves can be formed. These shock waves can interfere with the flow around a model in a wind tunnel because they can reflect off the nearby wind tunnel wall. In the supersonic flow regime if the model is sufficiently short and the Mach number sufficiently high, the reflected wave will miss the model and only influence the downstream flow, but if the reflected wave does interact with the model, a non true to free flight condition arises.

This fact becomes a problem, especially in the region around Mach 1, and thus is of concern when dealing with transonic flow. From about a Mach number of 0.75, depending on the aerofoil, a shock wave develops on the model and will form at about 90 degrees to the flow, and thus will extend to the wall and reflect back onto the model. Cancellation of this wave is necessary for accurate data to be obtained. An equal but opposite expansion wave must be formed at the boundary such that the interaction between the two cancels the reflected wave altogether. One way of achieving this is either by means of a slotted or perforated wall. Slotted walls have the advantage of reducing the need for velocity correction in wind tunnels as well as relieving the effects of choking. Since choking is a feature that is prominent during high Mach number testing, the slotted walls allow a model with a greater frontal area to be tested, thus reducing the limitations on model size slightly[1].

Besides the conventional methods of producing transonic flow in a wind tunnel, it is feasible to make use of the velocity induced in stationary air by means of the passage of a shock wave[2]. Instinctively, this option would mean extremely short duration testing times but at a significantly reduced cost when compared to more traditional means. A distinct advantage, however, is that the shock increases the density, meaning that significantly higher Reynolds numbers can also be achieved compared to the expansion processes of conventional facilities[3].

A shock tube is one of the more practical and useful type of apparatus for creating shock waves safely and repeatedly in an environment where their properties and associated flow characteristics can be measured and studied. However, there are very few of these in existence for the generation of steady transonic flows compared to conventional methods, because of the short test times and constraints on test-section size. They are, however, valuable as a teaching and demonstration facility in educational institutions because of the low cost of implementation.

[a] MSc(Eng) student
[b] Flow Research Unit, School of Mechanical, Industrial and Aeronautical Engineering, University of the Witwatersrand.
E-mail: beric.skews@wits.ac.za

 © SAIMechE All rights reserved.

1.1 The shock tube

A simple shock tube consists of two ducts initially at different pressures and separated by a frangible diaphragm as shown in the time-distance plot of figure 1.

Bursting of the diaphragm causes a shock wave to move down the low pressure section and an expansion wave up the other. At the same time a contact surface follows the incident shock wave, but at a lower Mach number, this being the interface between the shock heated gas on the right and the expansion cooled gas on the left. After some time, the incident shock wave will reflect off the downstream end of the shock tube and start propagating upstream towards the contact surface and the expansion waves. The point of first interaction between these features will be at the position of maximum testing time, since it relates to the position where the flow behind the incident shock wave has the greatest amount of time before being interfered with by the other features. The theoretical maximum testing time is the difference between the time at which the reflected wave interacts with the contact surface or expansion waves and the time at which the incident shock wave passes the position of maximum testing time. This will form the basis of the current facility.

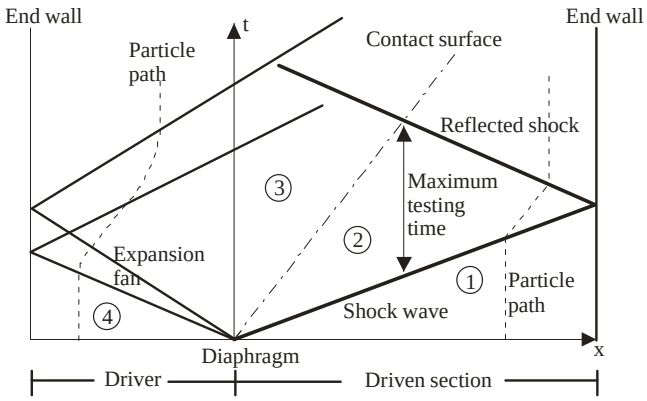

Figure 1: Simple shock tube wave diagram.

A slight increase in test time may be achieved by having a very weak diaphragm at the end of the driven section if an evacuated section is used, or to leave that end open. An expansion wave will then propagate back up the tube towards the test section at a much lower velocity than a reflected shock if the end wall were closed. It is not known if this technique has been previously employed but clearly safety issues such as hearing protection must be employed as the shock propagates outwards from the end of the tube.

The basic shock tube equations relating diaphragm pressure ratio and Mach numbers are[4]:

$$\frac{p_4}{p_1} = \frac{2\gamma_1 M_s^2 - (\gamma_1 - 1)}{\gamma_1 + 1}\left(1 - \frac{\gamma_4 - 1}{\gamma_1 + 1}\frac{a_1}{a_4}\left(M_s - \frac{1}{M_s}\right)\right)^{-2\gamma_4/(\gamma_4 - 1)} \quad (1)$$

$$M_2 = \frac{2(M_s^2 - 1)}{\left(2\gamma M_s^2 - (\gamma - 1)\right)^{0.5}\left((\gamma - 1)M_s^2 + 2\right)^{0.5}} \quad (2)$$

It is noted that for a fixed diaphragm pressure ratio the Mach number of the shock can be changed by changing the sound speed ratio, a_1/a_4, by either changing the gas or by preheating. Choice of gas could also change the specific heat ratio, thus also having an effect. For the current application air is used on either side of the diaphragm, due to the high cost of implementing either of these choices.

For a transonic tunnel in the context of flight speeds of commercial airliners the Mach numbers required of the facility are between 0.7 and 1.0. Thus, from figure 2 showing the dependence of post shock flow Mach number on shock Mach number for air, and the equations above, shock Mach numbers of the order from 1.6 to 2.0 are required. This corresponds roughly to diaphragm pressure ratios from 10 to 30. In view that the available maximum pressure available in the laboratory was just above 14 bar this meant the driven section had to be evacuated. It must be borne in mind that the theoretical values do not take into account losses and wave attenuation, thus higher pressure ratios than the theoretical will be needed.

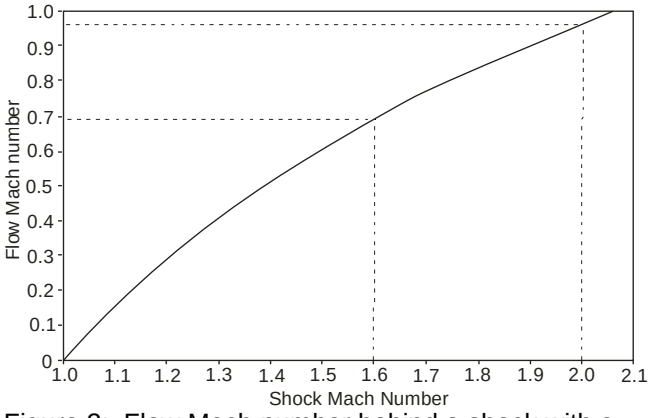

Figure 2: Flow Mach number behind a shock with a Mach number M_s moving into stationary gas

2. Facility design

2.1 Shock tube design

In view of the very limited budget available for this project it was required that, as far as possible, existing hardware and facilities should be employed. In addition, in order to increase the test time the tube should be as long as possible, as is evident from figure 1.

Although not ideal, the driven section was made from standard, industrial welded seam, rectangular section, steel tubing from a previous project. The sections available were thirteen 2 m long sections, two 1 m long sections and a single 0.6 m section. Each section had a flange welded to it and the flanges each contained two dowel pin holes to ensure accurate alignment once assembled.

The driver section was an existing pressure vessel made from three lengths of circular steel tubing with an outer diameter of 168.3 mm and wall thickness of 7.11 mm. Two lengths of 6 m and one length of 3.4 m made up the vessel. The total length of 15.4 m had been pressure tested and certified for a working pressure of 4 bar.

Due to the large shock wave Mach numbers required to produce the transonic flow, the vessel had to be recertified to a higher working pressure. The connecting flanges on the

http://www.saimeche.org.za (open access) © SAIMechE All rights reserved.

driver were upgraded to allow the vessel to be certified for a 15 bar working pressure. The 3.4 m section had a larger diameter flange welded to it to allow for connection to the driven section described above. One of the 6 m sections had a blanking flange to close the section off. In addition an accurately machined clean-up section of 3 m length and fitted with pressure transducer ports for triggering the imaging light source, was manufactured to be positioned upstream of the test section to even out the flow perturbations resulting from the roughness in the upstream commercial tubes.

The basic shock and expansion wave equations for the generation of wave diagrams such as that in figure 1 are available in software[5] (Kasimir3) which makes optimising of the test time using the available tube lengths simple, since various combinations of tube lengths could be tested for finding the best test time and corresponding position of the test section.

Considering all the constraints and the position of intervening obstructions, a driver length of 9.4 m and driven section of 36.6 m was selected. This was based on calculations for a mean flow Mach number of 0.83, which is in the middle of the desired range. The theoretical wave diagram for this case is shown in figure 3. This shows the calculated position of the test section and the corresponding test time. Repeat calculations show that for Mach numbers of 0.73, 0.83, and 0.93 the calculated test times at the optimal positions are 43, 35, and 29 ms respectively. This is regarded as sufficient for steady flow to be established. Although an extra 4 m of driven tube could be accommodated, this increased test time by about 3 ms and shifted the test position by 3 meters which was inconvenient regarding laboratory layout. For the same reason the test section was positioned 31.5 m from the diaphragm station which is satisfactory in view of the lower velocity of the returning wave from the end of the tube due to it being sonic because of the open end. A photograph of the tube is shown in figure 4, with views upstream and downstream taken approximately from the diaphragm station position.

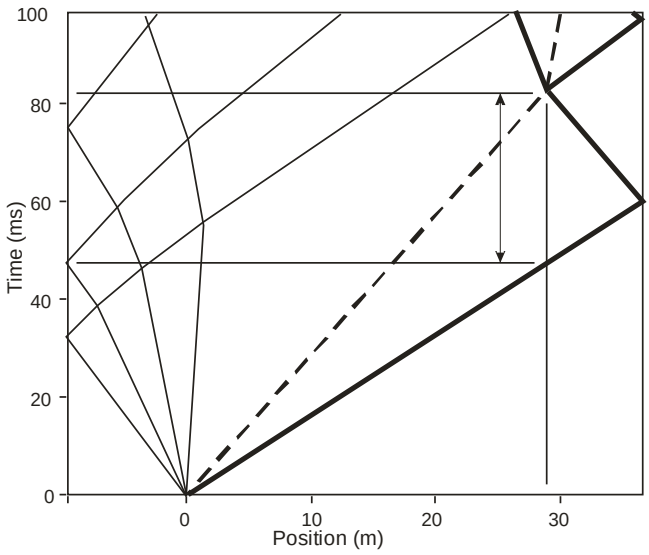

Figure 3: Theoretical wave diagram for given geometry

In addition to the aforementioned facts, it will be shown that the theoretically predicted behaviour differs from the actual behaviour of the shock tube due to attenuation effects. As a result, the theoretical testing position and testing time is simply a guide for an initial position for the test section with the actual position best determined experimentally.

In shock tube operation it is common to use a frangible diaphragm to separate the high and low pressure chambers. Bursting this diaphragm then initiates the flow. Because natural burst due to slowly increasing the pressure difference is unreliable in order to get repeatable results, the diaphragm is preloaded to a given pressure and then a pricker used to initiate the burst. A pneumatically operated pricker was used which as fired by opening a quick acting valve. Due to the high pressure ratios required to produce a shock wave with a high enough Mach number to induce transonic flow, a diaphragm thickness was needed that was capable of withstanding a pressure of 14 bar on the one side while a vacuum of up to 0.15 bar was drawn on the other side. After running a few experiments, it was found that two pieces of 300 micron sheet and two pieces of 100 micron sheet were required to hold the pressure difference, while at the same time not being too thick for the pricker to burst. It was further established that the two 100 μm sheets needed to be placed on the pricker side of the diaphragm. This meant that upon activation of the pricker, the 100 μm sheets would rupture and reduce the overall strength of the diaphragm sufficiently to cause the thicker 300 μm sheets to rupture.



Figure 4: Upstream and downstream views of the basic tube layout taken from about the diaphragm station

2.2 The test section and model

One of the most important features required of the test section is the ability to both cancel any reflected shock waves off the walls as well as minimise blockage effects in the wind tunnel. Studying literature on the way in which this has been achieved in larger scale wind tunnels revealed predominance in a slotted wall type layout. A plenum chamber is required to be installed behind the slotted wall in

http://www.saimeche.org.za (open access) © SAIMechE All rights reserved.

order to absorb the transmitted shock. The design was also arranged that different arrangements of slots in terms of the ratio of open to closed area could be incorporated. Due to slenderness of the slotted members, supports needed to be put in place to ensure that they do not vibrate or bend during testing. These supports also doubled as clamping regions to ensure that the spacing between the slots could be accurately maintained. The overall assembly is shown in figure 5.

The Perspex window is mounted in a hinged frame as shown in figure 6 and is held in place with three large bolts, two of which pass over the test section. Due to the requirement of evacuating the driven section to increase the shock wave Mach number, it needed to be sealed off from the atmosphere. It was decided that placing a very weak diaphragm at the end of the tube was the best solution. The diaphragm needed to be thick enough to hold the pressure difference from ambient pressure caused by the vacuum, but should burst upon contact with the incident shock wave. This resulted in an increase in test time due to the reflected wave being sonic. It was established that 50 μm sheet was capable of holding a vacuum of 0.1 bar on the one side, with Johannesburg's atmospheric pressure of 0.83 bar on the other side. It was also known that a diaphragm of this thickness would rupture with approximately 2.5 bar of pressure being applied to it, ensuring that the test section and tubing were not exposed to unnecessarily high pressures for an excessive amount of time. The diaphragm, in effect, acted likes a high volume flow rate, one-way valve making it ideal for use at this position in the tube.

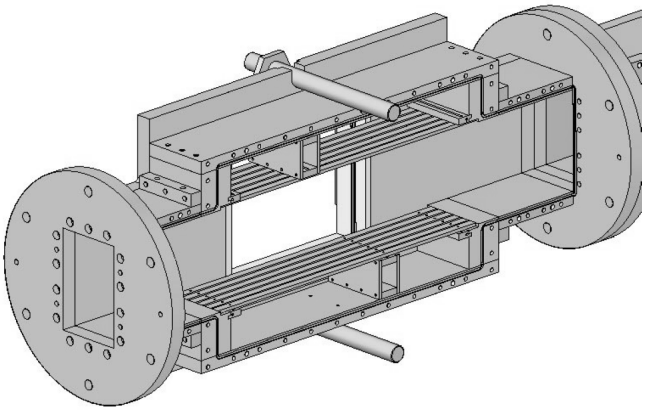

Figure 5: The basic test section design

Due to the fact that results from the initial commissioning testing would primarily be made up of photographs of the flow features, it was decided that an aerofoil with a large amount of known data be used.

The aerofoil chosen for testing was the RAE 2822 supercritical aerofoil, which has become a standard test case because of the amount of experimental data available and the number of numerical simulation cases showing good validation capabilities including the Fluent© [6] code used in the current investigation. This confidence in prediction accuracy meant that from a visual point of view, the transonic shock positions and shapes for the aerofoil, when subjected to transonic flow, would represent reality well. The profile of the 12 % thick RAE 2822 aerofoil is shown in figure 7.

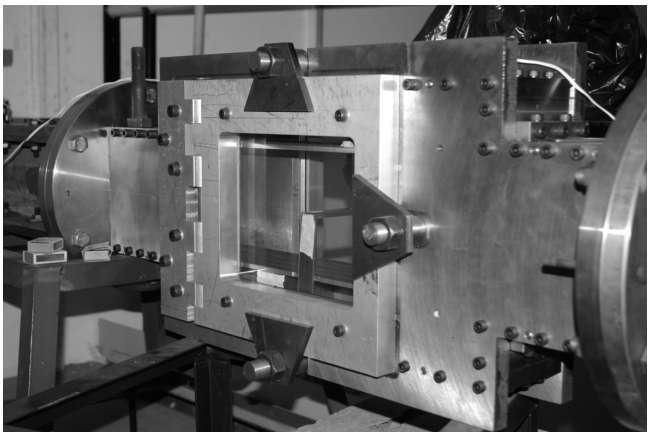

Figure 6: Photograph showing the door and clamping system



Figure 7: The RAE 2822 aerofoil profile

The aerofoil should span the full width of the test section such that effectively two-dimensional flow exists. Mounting the test piece with a sting type system meant that it would interfere with the flow around the model and create unnecessary complexity in the design. As a result it was decided to mount the test piece with vertical uprights on each side as shown in figure 8. The uprights were machined from 3 mm thick steel plates with a ten degree wedge machined into their leading edge to ensure that they interfere minimally with the flow.

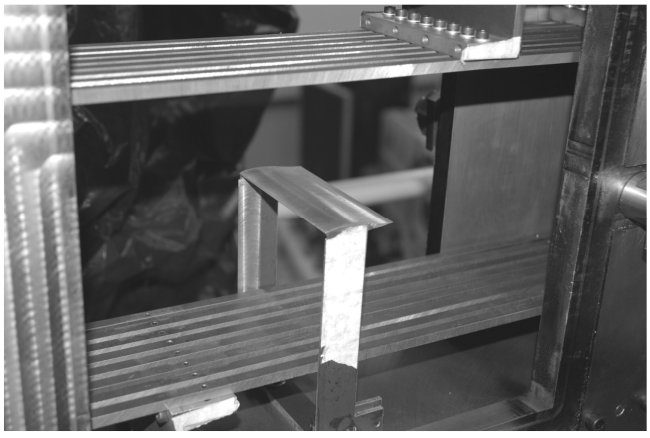

Figure 8: View of the test piece and mounting arrangement

This method has a few advantages and disadvantages. The advantages are that it would allow stable and secure mounting of the test piece, and the angle of attack would be easy to change by rotating the supports through adjustment under the grids. The main disadvantage is that only one surface of the test piece would be visible in an image, thus necessitating running the wind tunnel twice for each test condition, since the upper and lower surface would need to be tested separately by turning the test piece over. Different uprights were manufactured for each surface to ensure a smooth surface for the flow.

http://www.saimeche.org.za (open access) © SAIMechE All rights reserved.

2.3 Visualisation and instrumentation

The visualisation method used is known as schlieren imaging and it allows slight variations in density in a transparent medium to be observed which would otherwise be largely invisible to the unaided eye. It converts density gradient variations in a transparent medium into light variations which can be recorded. A common layout of optical components required to achieve the technique is shown in figure 9. A point source of light is cast upon a parabolic mirror positioned at the focal point of the mirror, resulting in a parallel beam of light being reflected from the mirror. This parallel beam then passes through the shock tube test section and is reflected by another parabolic mirror. A knife edge is placed at the focal point of the second mirror and is used to control the amount of light being received by the camera. Any deviation in the parallel beams caused by some change in density in the test region will alter that portion of the light passing to the camera. In the implementation used for the current facility the system had to be folded through a plane mirror since the tube was adjacent to the edge of a mezzanine floor where the facility was positioned.

Because of the short flow duration time a xenon flash light source of 2 µs duration was used to capture the flow.

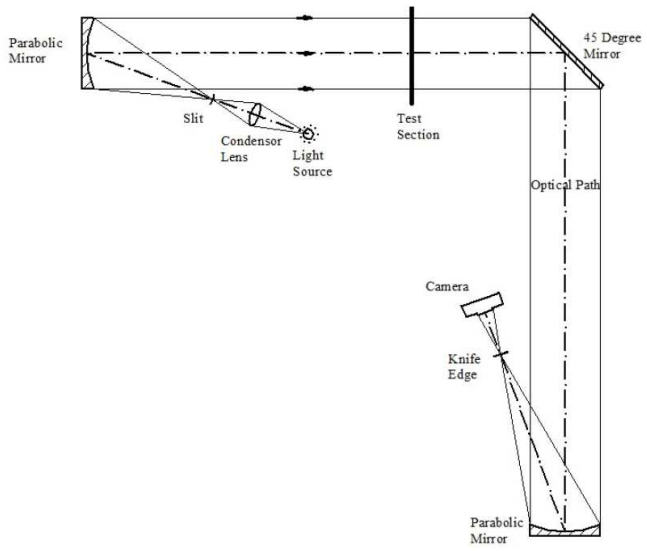

Figure 9: Schlieren optical system layout

Sensitive schlieren optical setups generally require that the test section windows be made from high quality but expensive glass. It was decided to use Perspex windows using sections from a plate of the material that were carefully selected in the schlieren beam so as to give minor striations. The results presented in this paper use these windows although this does result in minor background non-uniformity in the images.

Instrumentation for the commissioning tests consisted of two, fast response, PCB piezoelectric pressure transducers, connected to an amplifier. The amplified signals from the pressure transducers were sent to the data acquisition system for logging of the data. The upstream pressure transducers signal was split just before entering the data acquisition system with the second part of the signal connected to a delay box in order to trigger the light source at a given time delay. The data logged by the data acquisition system was used to calculate the Mach number of the incident shock wave by measuring the difference in arrival time of the incident shock at the two transducers.

2.4 Calibration

With a tube of the length used with the pressure transducers measuring Mach number some 31 meters from the diaphragm station, it was expected that shock attenuation would occur. A test run at a driver pressure of 14.2 bar into atmospheric pressure of 0.83 bar at 23º C, created a shock wave Mach number of 1.71 where theoretically a Mach number of 1.77 should have been produced. This meant that the flow behind the shock wave would be Mach 0.77, where theoretically it should be Mach 0.82. This attenuation is larger than expected based on conventional shock tubes in operation. Given the fact that the industrial steel tubing was not smooth inside, had a welded seam running the length of it, and the fact that over the 31 m, many tube joints existed, it was possibly unsurprising. Attempts at improving the situation by changing joint seals resulted in marginal improvement. Thus it became necessary to evacuate the driven section further, and thus increase the pressure ratio across the diaphragm, while leaving the driver pressure at the maximum available.

Tests were conducted at nominal flow Mach numbers of 0.73, 0.83, and 0.91 with the majority of the commissioning tests done at Mach 0.83.

2.5 Computational Fluid Dynamics

Due to the nature of this project more emphasis was placed on the results obtained experimentally than with the numerical results, these solely being used as a validation tool. The aerofoil section used during testing is the same type as Ansys Fluent© used to validate their numerical models for the transonic test range[6] because of the extensive amount of experimental data available, primarily those of Cook *et al.*[7]. There had been many other validation exercises such as that of Coakley[8] and is also documented in NASA's CFD validation collection[9]. These extensive exercises using different turbulence models, codes, and boundary conditions gives confidence in using the simulation results to establish flow conditions in the experiment.

The mesh layout shown in figure 10 is identical to that used during the Fluent© validation. The mesh extends to approximately ninety chord lengths from the aerofoil thus ensuring that the boundary of the mesh has no affect on the flow features. The mesh consists of quadrilaterals whose dimensions decrease as they approach the aerofoil in order to give greater definition where a large amount of detail is required.

The number of iterations that were completed for each test was dependent on the shape of the residual graphs and the solution was accepted as converged once the residuals indicated no major change with additional iterations. Convergence tended to be in the region of 15000 to 30000 iterations. The turbulence model was Spalart-Allmaras while the solution was set to steady state, two-dimensional with a coupled solver. Finally, the formulation was set to implicit.

http://www.saimeche.org.za (open access) © SAIMechE All rights reserved.

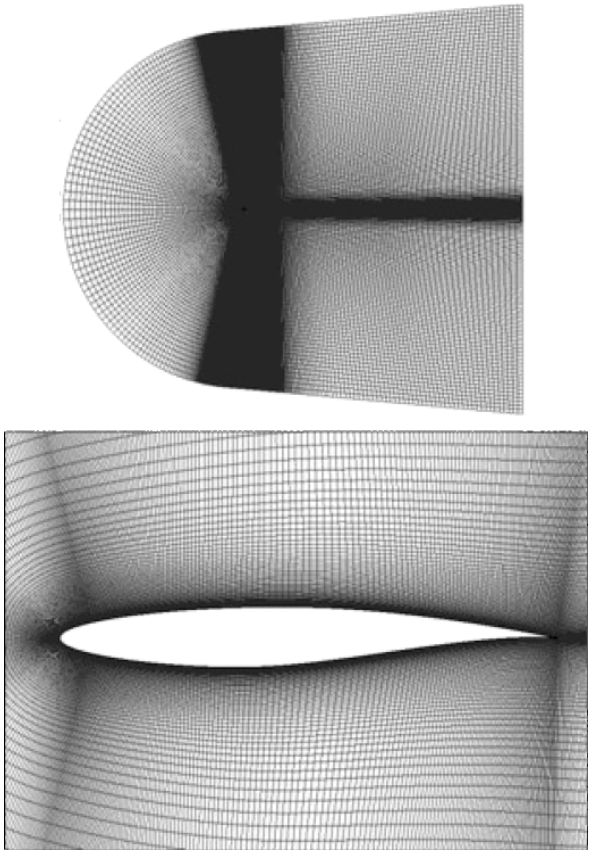

Figure 10: CFD mesh

It was recognised that flow velocity in the test section as determined from the incident shock velocity would be inaccurate due to attenuation and unsteady effects from factors such as boundary layer build-up. In the absence of sophisticated instrumentation within the test section the determination of the Mach number was done through comparison with the validated numerical results. It was found that this resulted in higher Mach numbers than the nominal values determined from the transducer shock transit measurement.

3. Results

3.1 Test results

A limited number of initial start-up tests were conducted to show that the wind tunnel was operating correctly. These were done at the nominal Mach number of 0.83, i.e. in approximately the middle of the transonic range. Angles of attack of 0, 2.79 and 5º were chosen with the bulk of the testing done at an angle of attack of 2.79º degrees, since this matches up with the angle of attack found most commonly in the literature, particularly relating to the validated numerical procedures. The first tests conducted were to ascertain the time taken for nominally steady flow to be established. These results are given in figure 11.

As the incident shock wave passed over the test piece (0.06 ms after striking the leading edge), a circular reflected wave propagates outwards from it. The incident shock wave is now no longer a vertical line but is slightly curved due to the obstruction it has encountered. The lower half of the incident shock wave also appears thicker than the upper half and this is because the lower half has been curved in the transverse plane due to the two uprights that it has passed through. A clear shear layer emanates from the intersection of the reflected wave and the incident wave, forming a typical Mach reflection pattern.

After 1.45 ms the incident shock wave is positioned 0.91 meters from the leading edge of the test piece. The reflected wave moving upstream is dissipating and the downstream transonic shock system is starting to form. At 4.45 ms the test section is largely free from the previously seen flow features and steady transonic shock waves are clearly visible on the trailing edge of the test piece. As shown later this pattern remains relatively stable until the return of the reflected shock wave from the end of the shock tube at about 40 ms.

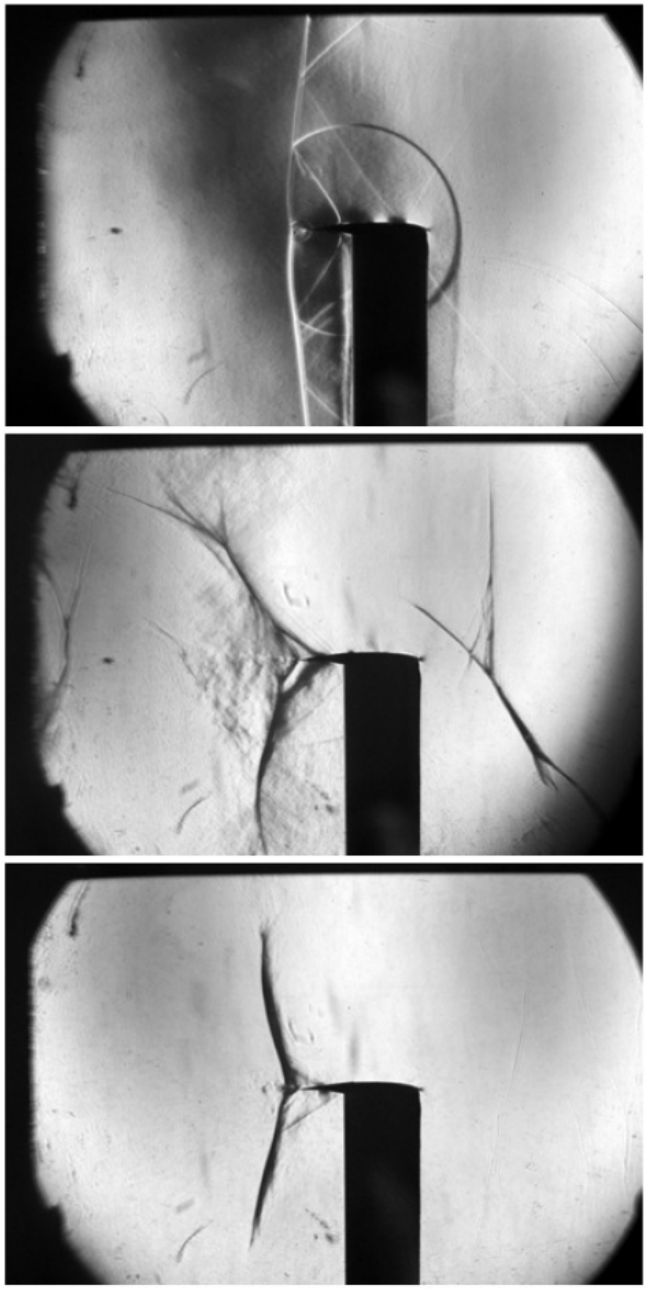

Figure 11: The start-up process with images taken at 0.06, 1.45 and 4.45 ms after shock arrival at the leading edge

http://www.saimeche.org.za (open access) © SAIMechE All rights reserved.

Tests were repeated with the test model in one orientation and then inverted in order to obtain flow images for both the upper and lower surface of the aerofoil. For the sake of clarity and in order to compare the test results with the numerical results, the upper and lower pictures were combined to produce a picture with no support mechanism.

Preliminary testing was performed for delay times starting soon after the passage of the shock wave over the model, and continued until it was clear the flow had become unsteady and unusable. The results are given in figure 12.

At 45 ms delay the flow becomes unstable on the upper surface as if the tunnel is choking. From the sequence shown in figure 12, it can be seen that the testing flow is established soon after the passage of the shock wave, remains semi-steady and then breaks down. The region where the flow is semi-steady is from approximately 10 ms to 40 ms. During this time duration, the transonic shock wave position on the test piece and the general shape of the shock wave varies by only a small amount. Some of this variance can be accounted for by the fact that each half of each image was obtained by means of a separate test and so some slight differences in Mach number are bound to occur.

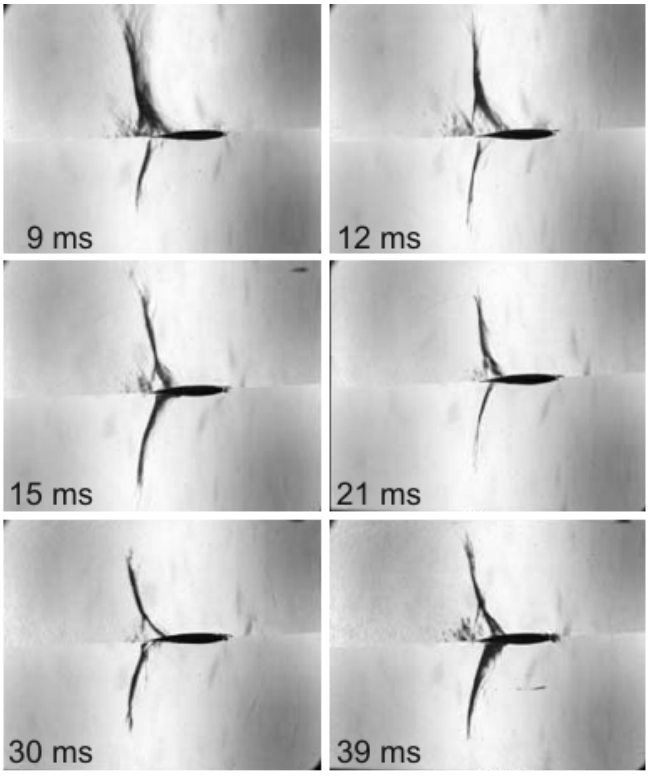

Figure 12: Effect of photograph delay time on the flow pattern

Each of the shock waves in this series of images has a lambda shock pattern displayed close to the surface of the test piece. This shock pattern forms due to the shock induced boundary layer separation that occurs on the test piece. At the point where the boundary layer separates, an oblique shock wave is formed. This oblique shock wave extends until it meets the normal shock wave which was the cause of the separation in the first place. At this point, a trailing shock forms and extends back towards the now separated flow, the formation of which is due to compatibility conditions downstream of the system needing to be satisfied. The finer details of this type of system are beyond the scope of this study, however, this type of system is known as a lambda shock system, due to the shape of the interaction of the three shock waves. Downstream of the lambda shock system, a significant turbulent region can be seen and this is due to the separation of the flow.

3.2 Comparison with numerical results

With the flow features surrounding the shock wave formation on the test piece clearly identified and understood, a comparison of the features displayed during physical testing can be made with those features predicted by the numerical results.

A test picture taken at approximately the middle of the testing time window was chosen for the comparison. The nominal testing Mach number was 0.83. A numerical result at this same Mach number was compared to the experimental image in order to compare the transonic shock wave shape, chord wise position and general flow features around the aerofoil. The numerical and experimental results were similar but not to a degree of accuracy that was regarded as acceptable since the numerical shock position was some 10 % of the chord length further up towards the leading edge. Since it is known that an increase in Mach number results in downstream movement of the transonic shock waves on the aerofoil, it is clear that the experimental result is at a Mach number that is higher than that of the simulation. The likely reason is that the boundary layer growth at the time of testing effectively reduces the cross sectional area of the section resulting in an increase in Mach number of the subsonic flow. This is not accounted for in the theoretical calculation of flow Mach number.

In order to establish the actual test Mach number, overlays of numerical results with an increasing Mach number was then created. The experimental result generated at 21 ms delay was chosen since it fell in approximately the middle of the testing time window. It was found that the numerical result at Mach 0.88 corresponded very well with the experiment as shown in figure 13. This was found to be the same for other tests at the same initial conditions. Furthermore from the comparisons in figure 12 it appears that the flow Mach number is relatively constant throughout the testing time window.

The numerical and experimental results contain similar features. Two defined transonic shock waves are clearly visible extending outwards from the upper and lower surfaces of the aerofoil into the surrounding flow. A turbulent wake region is also visible, as is a lambda shock pattern on the upper surface of the aerofoil. No clear lambda shock pattern is visible on the lower surface however, and this is made more evident by the fact that the turbulent wake region appears mainly to originate from the upper surface of the model. On the lower surface, since no lambda shock pattern is seen in either the experiment or simulation, no boundary layer separation is indicated.

Since the experimental setup did not contain any instrumentation that would allow the actual test Mach number to be known and since there is confidence that the numerical result is very accurate, based on previous validation[6], simply overlaying the numerical onto the

http://www.saimeche.org.za (open access) © SAIMechE All rights reserved.

experimental result and finding the closest match for the range of time delays meant that the experimental Mach number could be predicted with a fair degree of confidence.

3.3 Angle of attack results

A few tests were run with the aerofoil at an angle of attack of 5º .

Figure 14 gives the numerical result at an angle of attack of 5º and the corresponding experimental images taken at delay times of 9 and 21 ms. Flow again is established soon after the passage of the shock wave for reasonable test duration. The shock waves on the test piece are seen to be fairly thick in the images. This is due to the non-uniform nature of the test section as one passes from one window to the next, due to the slotted upper and lower walls causing in-plane bending of the shock wave.

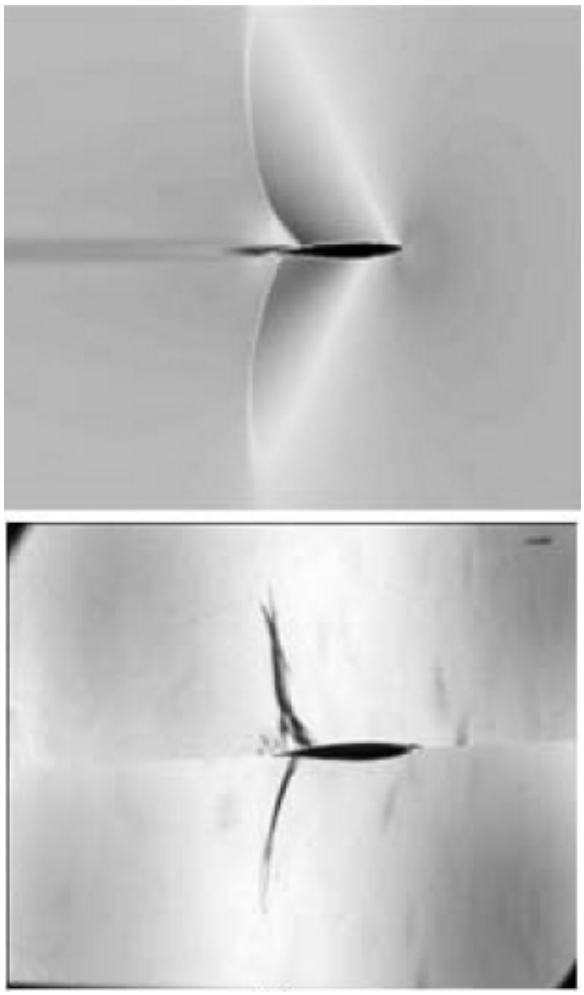

Figure 13: Numerical result at Mach 0.88 compared to experiment for an angle of attack of 2.79º

Generally, the shock waves formed on the upper surface of the model appear to extend further into the surrounding flow region in almost all of the images when compared to those seen during testing at 2.7º angle of attack. This is due to the fact that the higher angle of attack leads to a higher Mach number over the upper surface of the aerofoil which in turn leads to a stronger shock wave forming. This fact is further emphasised by the clear formation of lambda shock systems on the upper surface, whereas virtually no lambda shock system is seen on the lower surface. The lambda shock system is a result of the strong interaction between the normal shock wave formed on the surface and the boundary layer that is found along the surface. A clear

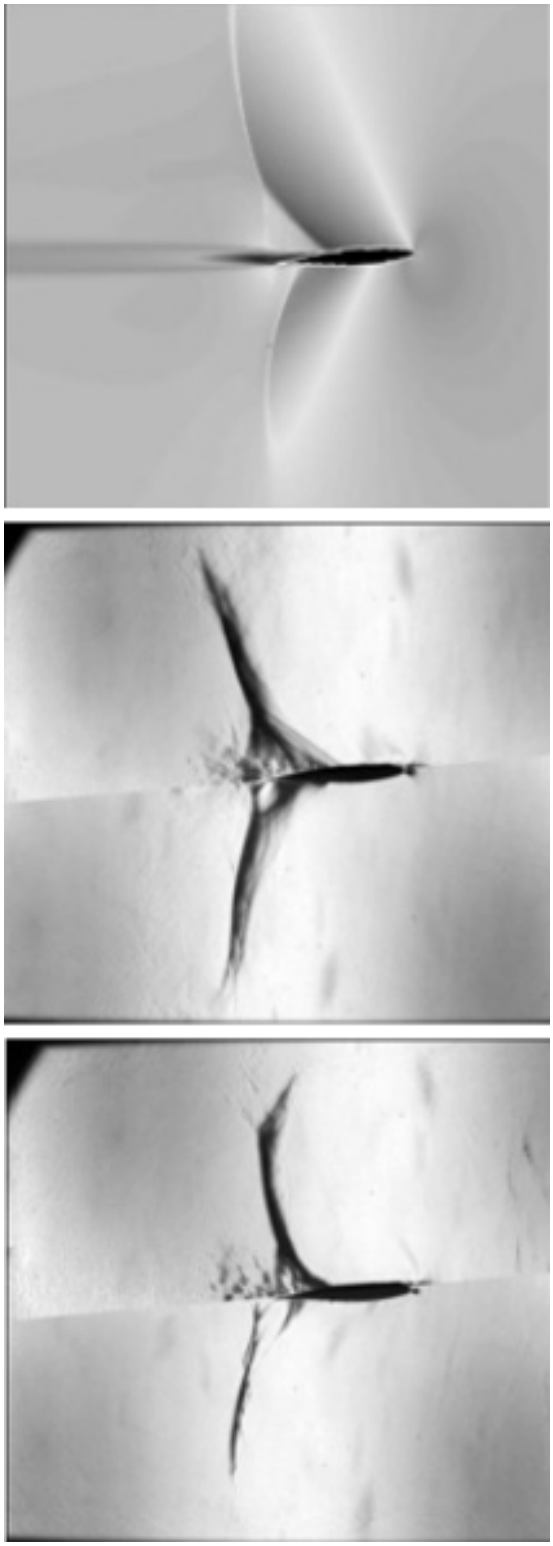

Figure 14: Numerical result at Mach 0.88 compared to experiment at 9 and 21 ms for an angle of attack of 5º

http://www.saimeche.org.za (open access) © SAIMechE All rights reserved.

wake region is seen resulting from the significant lambda shock system on the upper surface of the aerofoil whereas almost no wake is seen from the lower surface. This is due to the relative strengths of the shock waves on each surface and their resulting interaction with the boundary layer that is formed along each surface.

Whilst the experimental flow near the aerofoil corresponds well with the numerical simulation, the transonic shock waves curve less, or appear to bifurcate as they approach the upper and lower walls, indicating some influence. For these stronger shocks modification of the porous surfaces may need to be undertaken if better correspondence is required.

Once again, due to the lack of instrumentation in the test section of the wind tunnel, the actual Mach number of the flow can only be estimated. Thus, as done previously, numerical results were overlaid onto the experimental results in order to be able to accurately determine what the experimental Mach number was and again a Mach number of 0.88 was found to match most accurately with the results.

That said, there are some features contained in the higher angle attack results that are worth noting. From the numerical results, it is clear that the transonic shock waves extend much further from the aerofoil than in the results at a lower angle of attack. This fact means that the transonic shock waves formed during experimentation will be required to approach the boundary walls very closely. This is not an ideal feature since complex flow features are set up very close to the slotted walls and are likely to interact with the shock waves being formed. Inspecting the image in figure 14 at 9 ms delay, the transonic shock wave position on the aerofoil is almost identical to that predicted by the numerical results. In addition, the lambda shock system appears in the same position and is of the same proportion to that predicted numerically showing that the flow features around the aerofoil are being recreated correctly. The wake flow is clearly visible and as expected can be seen originating mainly from the upper surface of the aerofoil where the lambda shock system is found. A notable feature, however, is found as the upper transonic shock wave approaches the upper slotted wall in the bottom image. A slight kink is formed and is likely due to the complex interactions between the flow set up through the slotted wall boundary and the transonic shock wave itself, thus probably limiting the test times.

Similar agreement between tests and simulation occur at zero degrees angle of attack as shown in figure 15. It is noted that the shock on the lower surface is now much stronger than that on the upper surface due to an increase in flow Mach number over that surface. This results in strong lambda shock systems on both the upper and lower surfaces with the associated boundary layer separation.

3.4 Mach number effects

A few tests were conducted to ascertain the performance of the tunnel at different Mach numbers. For a Mach number of 0.75 fair correlation was obtained for the shock position on the upper surface as shown in figure 16 but a shock was found to occur on the lower surface even though this was not shown in the simulation. With these very weak waves it is evident that flow uniformity may be an issue and

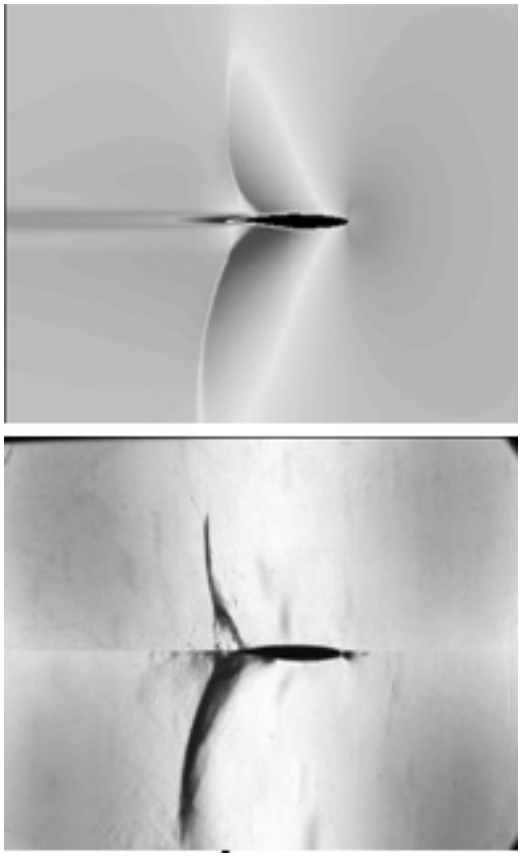

Figure 15: Numerical and experimental results at zero angle of attack

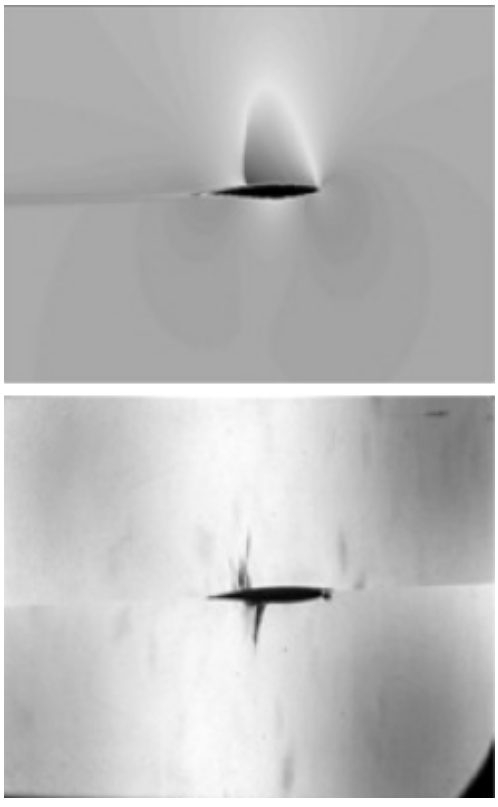

Figure 16: Numerical and experimental results at a Mach number of 0.75 and 2.79º angle of attack

sophisticated instrumentation will need to be implemented to accurately determine the Mach number profiles in the test section. On the other hand, for the higher Mach numbers it was found that at a Mach number of 0.91 the flow shows strong evidence of choking in the gap between the vertical model supports and thus gives an upper limit to the test range.

4. Conclusion

A small transonic facility has been developed based on shock tube technology in contrast to the more conventional technique using a nozzle supplied from a reservoir or compressor. It is shown to produce acceptable results for transonic flow demonstrations and small scale research projects in the Mach number range from 0.8 to 0.9. However for future work and further development of the facility, it is essential that it be further instrumented to gain a better understanding of the uniformity of the flow produced in the test section.

This paper is based on a MSc(Eng) project of the first author[10], which was partly supported by funding from the National Research Foundation.

References

1. *Goethert BH*, Transonic Wind Tunnel Testing. Pergamon Press, New York, 1961.
2. *Geiger, FW* and *Mautz CW*, The Shock Tube as an Instrument for the Investigation of Transonic and Supersonic Flow Patterns, Engineering Research Institute, University of Michigan, 1949.
3. *Olivier H, Reichel T* and *Zechner M*, Airfoil flow visualization and pressure measurements in high-Reynolds-Number Transonic Flow, *AIAA Journal*, 41, 8 ,1405-1412, 2003.
4. *Wright JK*, Shock Tubes, London, Methuen, 1961.
5. *Kasimir3*, Shock tube simulation program, *RWTH Aachen, 1993.*
6. *Fluent Inc.*, Fluent 6.3, Validation Guide, Fluent Inc. 2006.
7. *Cook PH, McDonald MA* and *Firmin MCP*, AEROFOIL RAE 2822 Pressure Distribution and Boundary Layer and Wake Measurements, AGARD Advisory Report No. 138, 1979.
8. *Coakley TJ*, Numerical simulation of viscous transonic airfoil flows, *AIAA 25th Aerospace Sciences Meeting*, 1987.
9. *NASA*, NPARK Alliance CFD verification and validation, *http://www.grc.nasa.gov/WWW/wind/* , 12 March 2013.
10. *Nash J*, Design, Construction and Calibration of a Transonic Wind Tunnel, MSc(Eng) dissertation, School of Mechanical, Industrial and Aeronautical Engineering, University of the Witwatersrand, 2012.